Biosensors and Bioelectronics 24 (2008) 297–305

Contents lists available at ScienceDirect

Biosensors and Bioelectronics

journal homepage: www.elsevier.com/locate/bios

AFM nanometer surface morphological study of *in situ* electropolymerized neutral red redox mediator oxysilane sol–gel encapsulated glucose oxidase electrochemical biosensors

Ana-Maria Chiorcea-Paquim, Rasa Pauliukaite, Christopher M.A. Brett, Ana Maria Oliveira-Brett*

Departamento de Química, Faculdade de Ciências e Tecnologia, Universidade de Coimbra, Rua Larga. 3004-535 Coimbra, Portugal

ARTICLE INFO

Article history:
Received 12 February 2008
Received in revised form 1 April 2008
Accepted 2 April 2008
Available online 11 April 2008

Keywords:
Oxysilane sol–gel
Atomic force microscopy (AFM)
Poly(neutral red)
Enzyme immobilisation
Biosensor

ABSTRACT

Four different silica sol–gel films: methyltrimethoxysilane (MTMOS), tetraethoxysilane (TEOS), 3-aminopropyltriethoxysilane (APTOS) and 3-glycidoxypropyl-trimethoxysilane (GOPMOS) assembled onto highly oriented pyrolytic graphite (HOPG) were characterized using atomic force microscopy (AFM), due to their use in the development of glucose biosensors. The chemical structure of the oxysilane precursor and the composition of the sol–gel mixture both influenced the roughness, the size and the distribution of pores in the sol–gel films, which is relevant for enzyme encapsulation. The GOPMOS sol–gel film fulfils all the morphological characteristics required for good encapsulation of the enzyme, due to a smooth topography with very dense and uniform distribution of only small, 50 nm diameter, pores at the surface. APTOS and MTMOS sol–gel films developed small pores together with large ones of 300–400 nm that allow the leakage of enzymes, while the TEOS film formed a rough and incomplete network on the electrode, less suitable for enzyme immobilisation. GOPMOS sol–gel film with encapsulated glucose oxidase and poly(neutral red) redox mediator, prepared by *in situ* electropolymerization, were also morphologically characterized by AFM. The AFM results explain the variation of the stability in time, sensitivity and limit of detection obtained with different oxysilane sol–gel encapsulated glucose oxidase biosensors with redox mediator.

1. Introduction

An electrochemical enzyme-based biosensor is an integrated receptor-transducer device that uses an immobilised enzyme layer as a biomolecular recognition element to detect the product of the reaction with a substrate, using electrochemical transduction (Harwood and Pouton, 1996).

Sol–gel techniques have been widely used for the preparation of organic–inorganic hybrid materials (Walcarius, 2001). The sol–gel network offers a non-aggressive enzyme immobilisation approach at room temperature, through physical entrapment rather than chemical bond formation, providing an attractive method for the development of biosensors (Pierre, 2004; Lev et al., 1997; Nadzhafova et al., 2007; Jia et al., 2007). They have been used for enzyme encapsulation not only for electrochemical (Tsionsky et al., 1994; Yao et al., 1995; Wang et al., 1996; Künzelmann and Böttcher, 1997; Li et al., 1998; Yao and Takashima, 1998; Lee et al., 2000a,b; Wang and Dong, 2000a; Wang et al., 2000; Rabinovich and Lev, 2001; Couto et al., 2002; Anitha et al., 2004; Han et al., 2005; Tan et al., 2005; Zhang et al., 2005) but also for optical biosensors (Noguer et al., 2002; Navas Diaz et al., 1998; van Unen et al., 2001; Martinez-Perez et al., 2003). Additionally, enzyme encapsulation in sol–gel may improve some properties in relation to other immobilisation methods, such as enzyme activity, biosensor sensitivity and longer linear response range to analyte (Pierre, 2004; Lev et al., 1997; Rabinovich and Lev, 2001).

Oxysilane chemical compounds possess attractive features including chemical inertness and physical rigidity, and can be easily organised into porous textures and network structures based on covalent Si—OR bonds. In particular, tetraoxysilanes (Künzelmann and Böttcher, 1997; Li et al., 1998; Yao and Takashima, 1998; Lee et al., 2000a,b; Wang and Dong, 2000a; Wang et al., 2000; Rabinovich and Lev, 2001; Anitha et al., 2004; Han et al., 2005; Noguer et al., 2002; Navas Diaz et al., 1998; Tsai et al., 2003; Kauffmann and Mandelbaum, 1996), and trioxysilanes, such as 3-aminopropyltriethoxysilane (APTOS) (Wang et al., 2000; Couto et al., 2002), 2-(3,4-epoxycyclohexyl)-ethyltrimethoxysilane (Wang and Dong, 2000a; Wang et al., 2000) and methyltrimethoxysilane (MTMOS) (Lev et al., 1997; Rabinovich and Lev, 2001; Couto et al.,

* Corresponding author. Tel.: +351 239 835295; fax: +351 239 835295.
E-mail address: brett@ci.uc.pt (A.M. Oliveira-Brett).

0956-5663/$ – see front matter © 2008 Elsevier B.V. All rights reserved.
doi:10.1016/j.bios.2008.04.001

2002; Han et al., 2005; Tan et al., 2005), have been the oxysilanes most exploited for enzyme entrapment.

Electrochemical sol–gel biosensors have been prepared on different electrode materials (Pierre, 2004; Lev et al., 1997; Nadzhafova et al., 2007; Jia et al., 2007), although carbon electrodes, in particular graphite (Barroso-Fernandez et al., 1998), screen printed (Noguer et al., 2004), carbon paste (Wang et al., 1996; Li et al., 1998; Pamidi et al., 1997), glassy carbon (Nadzhafova et al., 2007; Wang and Dong, 2000a) and carbon composite (Teh et al., 2004), have received increased attention due to their wide positive potential window, hardness, mechanical stability and low porosity. Additionally, carbon represents a very good choice for enzyme immobilisation given the good compatibility between the enzyme layer and the electrode substrate.

Despite the extensive use of electrochemical sol–gel enzyme biosensors, the formation and stability of the sol–gel network on the carbon electrode surface are still not well understood. Atomic force microscopy (AFM) is a direct probing technique that can give important information concerning the interfacial and the conformational properties of sol–gel films. In particular, magnetic AC mode (MAC mode) AFM imaging allows the investigation of molecules loosely attached to the substrate, especially useful in the case of conducting surfaces of electrochemical sensors.

Depending on the required application, the control of the immobilisation of the enzymes and of the redox mediators in close proximity to the electrode is the most important step in the design and construction of efficient electrochemical enzyme biosensors, directly influencing the enzyme's three-dimensional structure, stability, specificity and activity.

The aim of this work was to perform an AFM morphological study to enable the understanding at the nanometer level of the modified electrode surface conformation after *in situ* electropolymerization of neutral red redox mediator and oxysilane sol–gel encapsulation of glucose oxidase in order to establish the optimal combination of sol–gel matrix, for encapsulating glucose oxidase, and of the redox mediator on carbon electrode substrates, to improve the enzymatic properties of glucose electrochemical biosensors. The systematic MAC mode AFM study at room temperature of the adsorption and of the conformational changes of different sol–gel films prepared on a highly oriented pyrolytic graphite (HOPG) electrode substrate using four different oxysilane precursors: 3-aminopropyltriethoxysilane, tetraethoxysilane (TEOS), methyltrimethoxysilane, and 3-glycidoxypropyl-trimethoxysilane (GOPMOS) was carried out. Different steps involved in the construction of a glucose biosensor assembled through the modification of an HOPG electrode with poly(neutral red) (PNR) redox mediator by electropolymerization followed by coating with sol–gel encapsulated glucose oxidase (GOx) were investigated.

2. Experimental

2.1. Materials and reagents

Four oxysilane precursors were used in silica sol–gel preparation: APTOS and TEOS obtained from Fluka, MTMOS and GOPMOS, obtained from Aldrich.

Neutral red (NR) monomer (N^8,N^8,3-trimethylphenazine-2,8,-diamine), 65% dye content was from Aldrich and glucose oxidase from *Asperigillus niger* (EC 1.1.3.4) was obtained from Sigma.

The supporting electrolyte solution used was pH 5.5 0.1 M phosphate buffer (PB), prepared from sodium dihydrogenphosphate and disodium hydrogenphosphate (Riedel-de-Haën). All solutions were prepared using analytical grade reagents and purified water from a Millipore Milli-Q system (conductivity $\leq 0.1\ \mu S\,cm^{-1}$).

The pH measurements were carried out with a Crison micropH 2001 pH-meter with an Ingold combined glass electrode. All experiments were done at room temperature ($25 \pm 1\ ^\circ C$).

The HOPG grade ZYB of 15 mm × 15 mm × 2 mm dimensions, from Advanced Ceramics Co., was used as a substrate. The HOPG was freshly cleaved with adhesive tape prior to each experiment and imaged by MAC mode AFM in order to establish its cleanliness.

2.2. Preparation of sol–gel film modified carbon electrodes

The HOPG electrode was modified by sol–gel thick films using four different procedures.

2.2.1. Procedure 1: APTOS, TEOS, MTMOS and GOPMOS sol–gel-modified HOPG

The sol–gel solutions were prepared by mixing the chosen oxysilane and water or pH 5.5 0.1 M PB (in the case of MTMOS) using previously optimised ratios (Pauliukaite and Brett, 2005; Pauliukaite et al., 2006): APTOS:H_2O: 220:580 μL; TEOS:PB: 180:620 μL, MTMOS:H_2O: 180:620 μL and GOPMOS:H_2O: 200:600 μL.

To each mixture, 2 μL of 1 M HCl solution was added. The solutions obtained were intensively stirred for a few minutes and then sonicated for 15 min. Following this, the solutions were heated in a hot air stream (~70 °C) for 30–50 min (except MTMOS, since in this case the components of the mixture separated and gelled rapidly after heating for a few minutes). Using this procedure, the alcohol formed during hydrolysis of the oxysilanes (Ferrer et al., 2002) evaporated until the solutions lost 40% of their volume. The mixtures were then left for an hour at room temperature to cool down and the pH was adjusted to 5.5 if necessary. A 50 μL aliquot of the appropriate oxysilane solution was placed on the freshly cleaned HOPG electrode, left 5 min (or 1 h in the case of TEOS), the excess of solution then was removed and the HOPG electrode was left for sol–gel film formation in a sterile atmosphere, at 4 °C for 3 days. The sol–gel film modified HOPG electrodes were imaged by AFM in air.

2.2.2. Procedure 2: GOPMOS–GOx-modified HOPG

A volume of 50 μL of GOPMOS mixture as obtained in *Procedure 1* was mixed with 15 μL of GOx (10%) solution in pH 5.5 0.1 M PB solution, vortex-mixed at 10 Hz during 30 s, and left for 2 h to equilibrate. To avoid denaturation of the enzyme, no alcohol was added to the sol–gel solutions, and vortex mixing was used for homogenisation of the sol–gel solution instead of sonication. A 50 μL aliquot of GOPMOS–GOx solution was then deposited on the HOPG electrode for 5 min, the excess of solution was removed and the HOPG electrode was left for sol–gel formation in a sterile atmosphere, at 4 °C for 3 days.

2.2.3. Procedure 3: PNR-modified HOPG

A PNR-modified HOPG electrode was prepared by electrochemical polymerization from a 1 mM NR monomer aqueous solution, in pH 5.5 0.05 M PB plus 0.1 M KNO_3, by potential cycling 10 times from −1.0 to +1.0 V, vs. Ag quasi reference electrode (AgQRE), at a potential sweep rate of 50 mV s^{-1}. The PNR-modified HOPG electrode was left for one day in air at room temperature before use.

2.2.4. Procedure 4: PNR/GOPMOS and PNR/GOPMOS–GOx-modified HOPG

A volume of 50 μL of GOPMOS sol–gel mixture, *Procedure 1*, or GOPMOS–GOx solution, *Procedure 2*, was deposited for 5 min on the PNR-modified HOPG electrode, *Procedure 3*, the excess of solution was removed and the electrode was left for sol–gel film formation at 4 °C for 3 days.

2.3. Methods and instruments

For electrochemical polymerization of neutral red on the HOPG electrode surface, a one-compartment Teflon cell of approximately 12.5 mm internal diameter was used, holding the HOPG working electrode on the bottom of the cell. A Pt wire counter electrode and an AgQRE were placed in the cell, dipping approximately 5 mm into the solution. Potential cycling was done using a μAutolab running with GPES 4.9 software, Eco-Chemie, Utrecht, The Netherlands.

The various sol–gel- or PNR/sol–gel-modified HOPG electrodes were imaged by AFM in air. AFM was performed with a PicoSPM controlled by a MAC mode module and interfaced with a PicoScan controller from Molecular Imaging Corp., Tempe, AZ. All the AFM experiments were performed with a CS AFM S scanner with a scan range 6 μm in *x*–*y* and 2 μm in *z* direction, from Molecular Imaging Corporation. Silicon type II MAClevers of 225 μm length, 2.8 N m^{-1} spring constants and 60–90 kHz resonant frequencies in air (Molecular Imaging Co.) were used. All images (256 samples/line × 256 lines) were taken at room temperature; scan rates 0.8–1.6 lines s^{-1}. When necessary, MAC mode AFM images were processed by flattening in order to remove the background slope and the contrast and brightness were adjusted.

Section analyses and root-mean-square (RMS) roughness (i.e. the standard deviation of the surface height) measurements were performed with PicoScan software version 5.3.1, Molecular Imaging Co. All the RMS roughness measurements were measured after 1st order flattening was performed. Microcal Origin version 6.0 was used to calculate the mean values of the measured topographical features and standard deviations.

3. Results

AFM was employed for the morphological characterization of the HOPG electrode surface modified by films of sol–gel with encapsulated enzyme and by redox mediator. MAC mode AFM was used

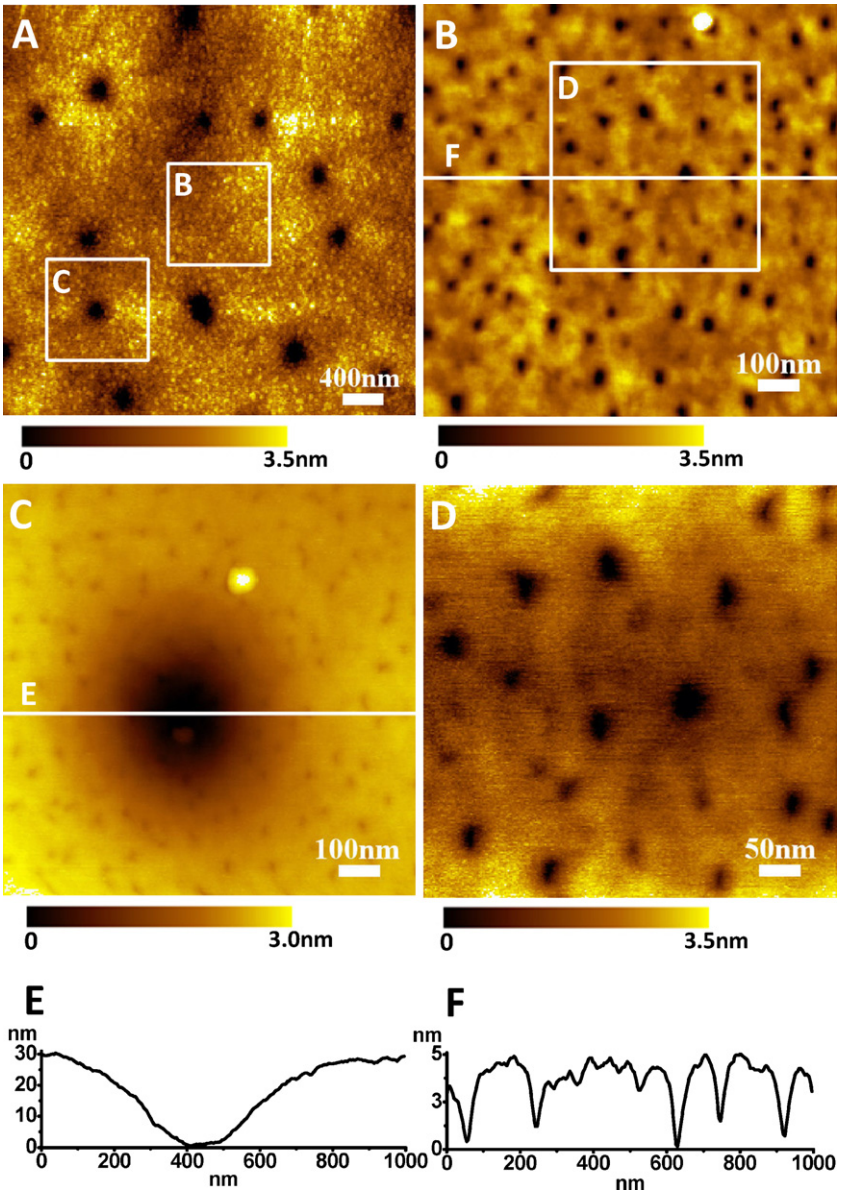

Fig. 1. MTMOS-modified HOPG electrode. (A–D) MAC mode AFM topographical images in air; (B–D) higher magnification topographic images corresponding to the white squares: (B and C) in image (A) and (D) in image (B), and (E and F) cross-section profiles through the white lines in images (B) and (C).

throughout this study, because is a non-damaging technique that allows the visualisation of the sol–gel films weakly attached on the carbon electrode surface. MAC mode uses a solenoid placed under the sample holder to cause a magnetically coated AFM cantilever to oscillate near its resonant frequency. As it scans the sample, the AFM tip oscillates and touches the sample surface only at the bottom of this oscillation. The control of the cantilever increases considerably, which enables operation at smaller oscillation amplitudes even in air, the lateral forces being better eliminated. The AFM topographic images can provide information about the roughness of the film and the size of the pores can be measured. The HOPG electrode surface used in this study is extremely smooth, presenting an RMS roughness of less than 0.06 nm, as calculated from a typical 1000 nm × 1000 nm scan size AFM image in air (Chiorcea and Oliveira Brett, 2004), which enables a correct evaluation of the smoothness of the different sol–gel films.

3.1. AFM characterization of HOPG modified with different sol–gels

The morphological characteristics of MTMOS, TEOS, APTOS and GOPMOS sol–gel-modified HOPG surfaces were investigated by AFM in order to understand the process of formation of silica networks during sol–gel formation. The morphological structures and thickness of dry sol–gel films depend on the chemical structure of the oxysilane precursor material, affecting both the properties and the enzyme encapsulation capacity of sol–gel-enzyme layer biosensors.

The sol–gel synthesis of nanostructured silica films requires the preparation of sol–gel mixtures from their chemical precursors, followed by placing a chosen volume onto the HOPG electrode surface, as described in *Procedure 1*. The process of the formation of sol–gel films from the oxysilane precursors involves two steps, sol–gel hydrolysis and polycondensation reactions, this second step being responsible for SiO_2 lattice formation for efficient enzyme encapsulation.

The first sol–gel film imaged was MTMOS, which presents the simplest chemical structure with three methoxy groups and one methyl group in tetrahedral positions around the Si atom. Sol–gel polymerization of MTMOS led to the formation of a three-dimensional network uniformly covering the electrode, Fig. 1. Large pores were distributed randomly on the top of the sol–gel films, Fig. 1A and C, but using higher magnification topographic images, very small pores are easily seen, Fig. 1B and D. The morphology of the MTMOS film was imaged on two different areas, corresponding to the white quadrants in Fig. 1A: from an apparently smooth part of the MTMOS film, Fig. 1B, and from an area where one big pore was imaged, Fig. 1C. The very small pores in Fig. 1B, initially masked by the presence of the big ones in Fig. 1A, can be clearly recognised. The structure of these small pores was even better evidenced using the AFM zoom in Fig. 1D. Section analysis inside the images showed that the large pores presented approximately 300–400 nm diame-

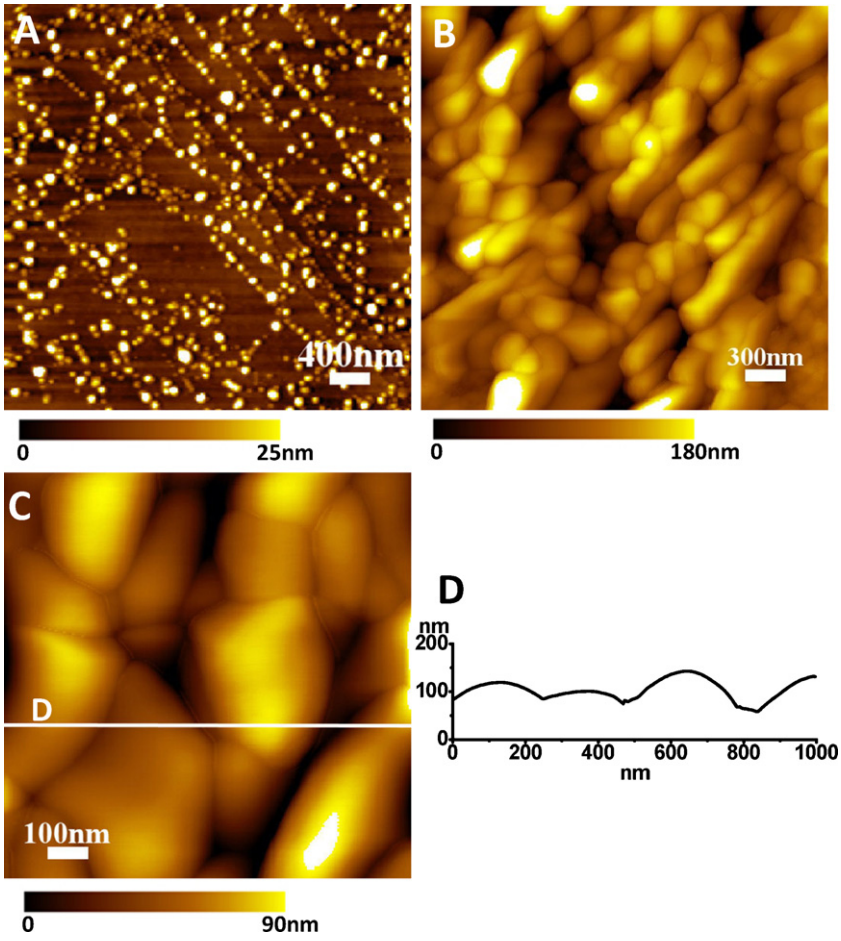

Fig. 2. TEOS-modified HOPG electrode, obtained after deposition contact times: (A) 5 min and (B–D) 1 h. (A–C) MAC mode AFM topographical images in air and (D) cross-section profile through the white line in image (C).

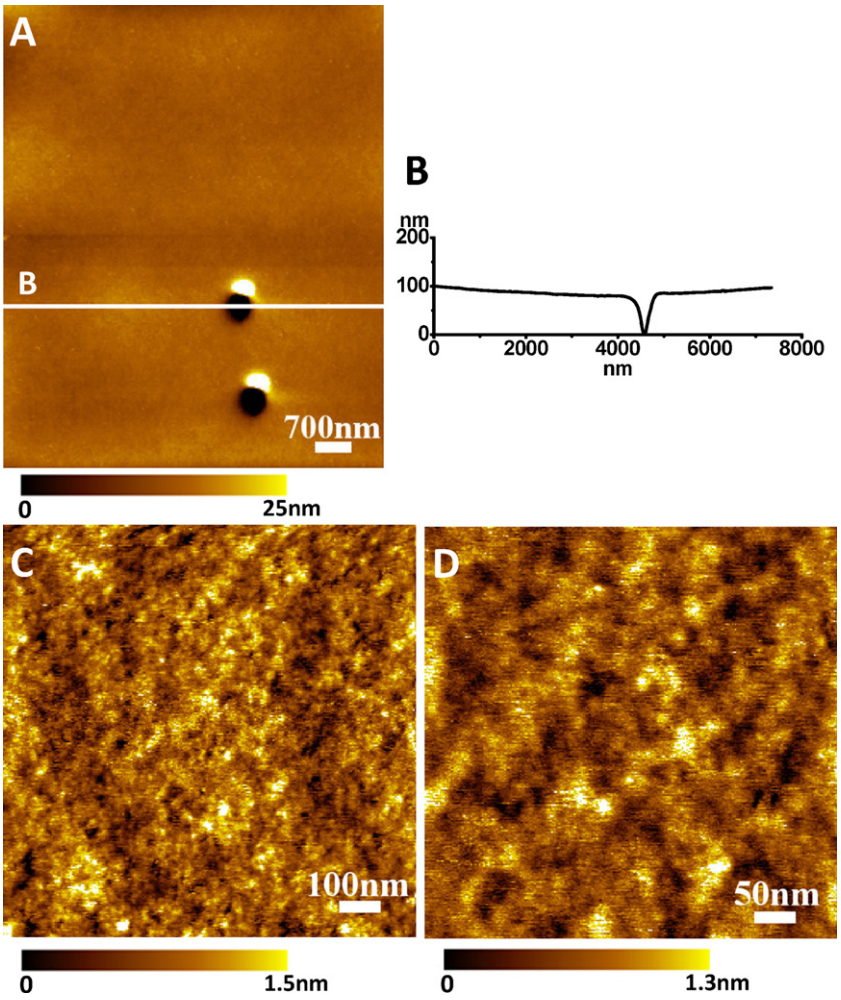

Fig. 3. APTOS-modified HOPG electrode. (A, C and D) MAC mode AFM topographical images in air and (B) cross-section profile through the white line in image (A).

ter, while the smallest ones were 40–80 nm in diameter, Fig. 1E and F. However, the AFM tip is not sufficiently long and narrow and the depth of the pore cannot be evaluated. In the 1000 nm × 1000 nm area where one big pore is present, Fig. 1C, the MTMOS film presented an RMS roughness of 5.5 nm, while in the smoother part of the sol–gel network, where only small pores were clearly visible, the RMS roughness was only approximately 1.0 nm.

The second sol–gel film imaged was TEOS, a sol–gel precursor with four ethoxy groups around the Si atom. After 5 min contact time on the carbon electrode surface, TEOS demonstrated poor adhesion, when compared with MTMOS, so that, after removal of the excess sol–gel solution, a low degree of surface coverage of the electrode was observed, Fig. 2A. The TEOS sol–gel appeared in the AFM images as globular aggregates, of very non-uniform size, from 5 up to 40 nm height. The RMS roughness measured in a 1000 nm × 1000 nm size image was approximately 5.2 nm. Increasing the contact time from 5 min to 1 h resulted in the formation of a very thick and rough silica film, as can be seen in Fig. 2B and C, due to polymerization of the TEOS precursor during a much longer time. The film had large peaks and valleys, with heights up to 150 nm, Fig. 2D, and an RMS roughness of 31.7 nm for a 1000 nm × 1000 nm size area.

As described below, films formed from either APTOS or GOPMOS precursors presented more complex morphologies when compared with the films formed from MTMOS or TEOS precursors.

APTOS has three ethoxy groups and an aminopropyl group and can form strong covalent bonds with organic and inorganic compounds (Zhou et al., 1999), being a good candidate for enzyme encapsulation. The formation of a very smooth APTOS film with only a few, very large pores of diameter between 600 and 800 nm is shown in Fig. 3A and B. In general, for the maximum 7000 nm × 7000 nm scan size of the CS AFM scanner, only one or two big pores were observed, Fig. 3A. Higher resolution AFM images, Fig. 3C and D, also demonstrated the existence of many small pores of 20–60 nm in diameter, Fig. 3C and D. The RMS roughness of a typical 1000 nm × 1000 nm scan size image, with only small pores, was of 0.4 nm, Fig. 3C, while a value of 2.1 nm was calculated in a 1000 nm × 1000 nm area where one big pore was imaged (image not shown).

GOPMOS has the most complex structure of the oxysilanes used in this study, presenting three methoxy groups, a three carbon chain and a glycidoxy group. The epoxy ring at the end of the glycidoxy group displays chemical activity and can react with other active groups, e.g. the amino group, of other compounds (Gao et al., 2004). The formation of sol–gel from GOPMOS precursor led to the formation of a uniform thin film that completely covered the electrode, Fig. 4A, with a very smooth topography of RMS roughness approximately 0.4 nm, Fig. 4B. The morphology of the GOPMOS film surface did not present big pores in the AFM images, only small pores of less than 50 nm in diameter, Fig. 4C and D.

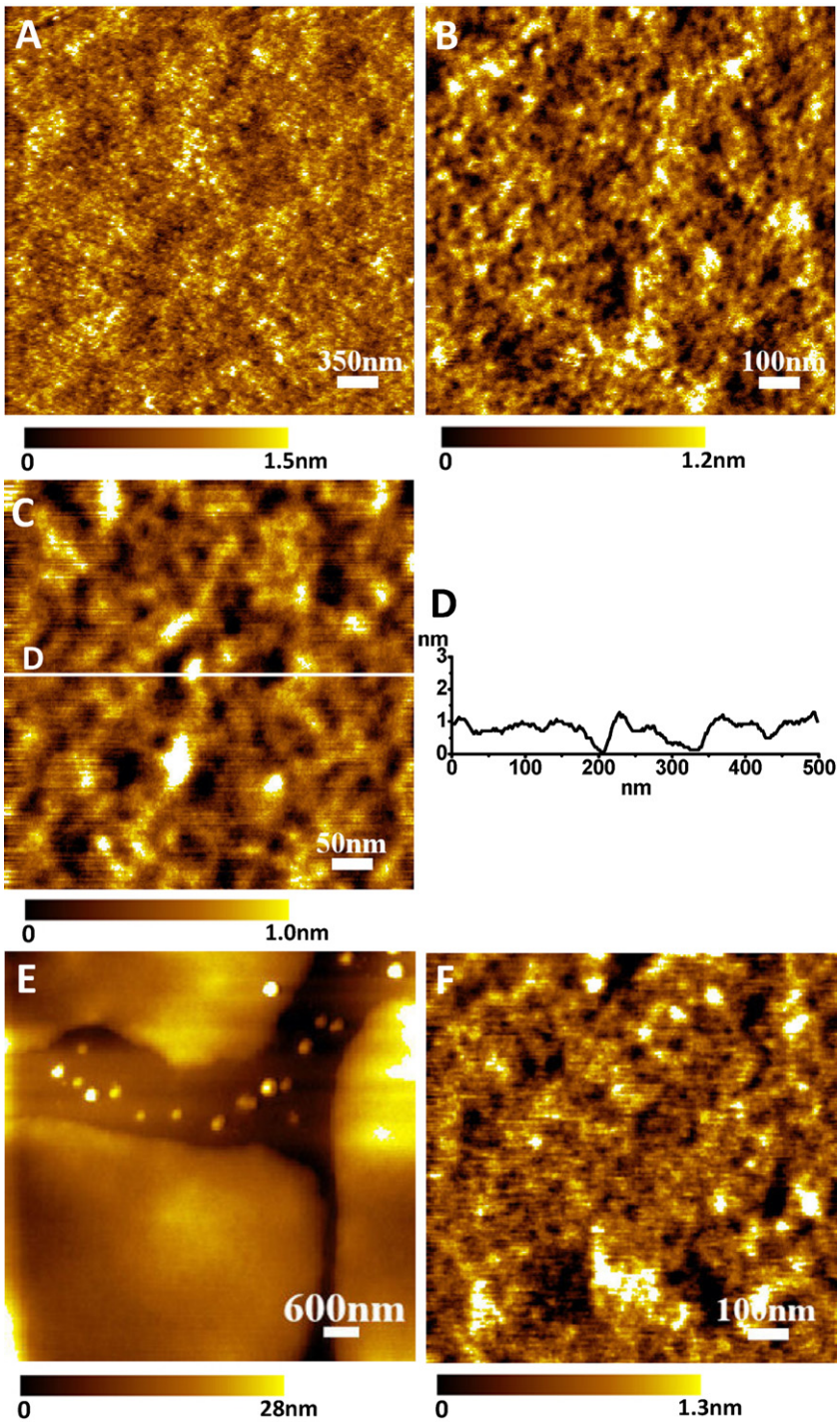

Fig. 4. (A–D) GOPMOS-modified HOPG electrode and (E and F) GOPMOS–GOx-modified HOPG electrode. (A–C, E and F) MAC mode AFM topographical images in air and (D) cross-section profile through the white line in image (C).

3.2. AFM characterization of a GOPMOS–GOx glucose biosensor

Given the current interest in the improvement and development of novel glucose electrochemical biosensors on carbon electrode substrates, the influence of encapsulating GOx into the GOPMOS sol–gel polymeric network was also evaluated by AFM. GOPMOS-enzyme biosensors were chosen since they have shown the lowest detection limit and the best sensitivity (Pauliukaite and Brett, 2005; Pauliukaite et al., 2006), taken together with the GOPMOS sol–gel film's smoother and more homogeneous morphology, Fig. 4A–C.

A GOPMOS–GOx mixture was deposited onto the surface of the HOPG electrode, as described in *Procedure 2*, and investigated by AFM in air, Fig. 4E and F. Large-scale AFM showed very flat domains, separated by areas with the enzyme aggregated in big spherical particles, which suggests an inhomogeneous distribution of the enzyme in the sol–gel, Fig. 4E. However, high-resolution images of the flat domains demonstrated the formation of a smooth GOPMOS–GOx film, Fig. 4F, similar to what was observed for the GOPMOS sol–gel film, Fig. 4B. Nevertheless, the RMS roughness of the mixed network increased from 0.4 nm, in the case of only

GOPMOS, Fig. 4A, to 1.3 nm, which can be ascribed to the effect of the entrapment of enzyme molecules inside the GOPMOS network pores, Fig. 4F.

3.3. AFM characterization of PNR-modified HOPG

Glucose electrochemical biosensors use appropriate redox mediators for improved selectivity. Poly(neutral red) has been used in the construction of various biosensor assemblies for glucose detection (Pauliukaite and Brett, 2005; Pauliukaite et al., 2006), a preferred redox mediator because it shows good adhesion on carbon electrodes, when compared with other mediators (Barsan et al., 2008). Thus, a PNR-modified HOPG electrode surface was morphologically characterized by AFM, Fig. 5A and B.

PNR-modified HOPG was obtained by electropolymerization of the NR monomer on the electrode surface, as described in *Procedure 3*, see Fig. 5C. The irreversible oxidation of the NR monomer, initially at $E^1_{pa} = +0.8$ V vs. AgQRE, changes in potential and peak shape in successive scans, due to the NR electropolymerization on the electrode surface (Pauliukaite et al., 2007). The redox couple 2_c–2_a, centred between −0.7 and −0.5 V, vs. AgQRE, is due to NR-leuco (NRH_2)-NR reduction–oxidation, clearly showing the polymer growth with increasing number of cycles; the reduction peak 2_c is shifted to more positive potentials, related to branching of the PNR and changing of the surface structure. The prepared PNR-modified HOPG electrode was left for 1 day in air at room temperature before use.

As can be observed in the AFM images, a thick PNR film grew on the surface of the HOPG electrode, Fig. 5A and B, presenting a granular topography with 2–10 nm height globular aggregates, Fig. 5D. The average RMS roughness in 1000 nm × 1000 nm scan size images was 1.4 nm.

3.4. AFM characterization of a PNR/GOPMOS–GOx glucose biosensor

Following the independent characterization of the PNR-modified HOPG electrode and identification of the GOPMOS–GOx-modified HOPG electrode as being that which shows the less rough and porous morphology (Pauliukaite and Brett, 2005; Pauliukaite et al., 2006), the morphology of a GOPMOS sol–gel encapsulated GOx film on the surface of a PNR-modified HOPG electrode was investigated.

A GOPMOS sol–gel film was left to dry on top of a PNR-modified HOPG electrode as described in *Procedure 4*. The film presented a very smooth topography, Fig. 6A and B, similar to that obtained for the GOPMOS immobilised directly onto the HOPG electrode,

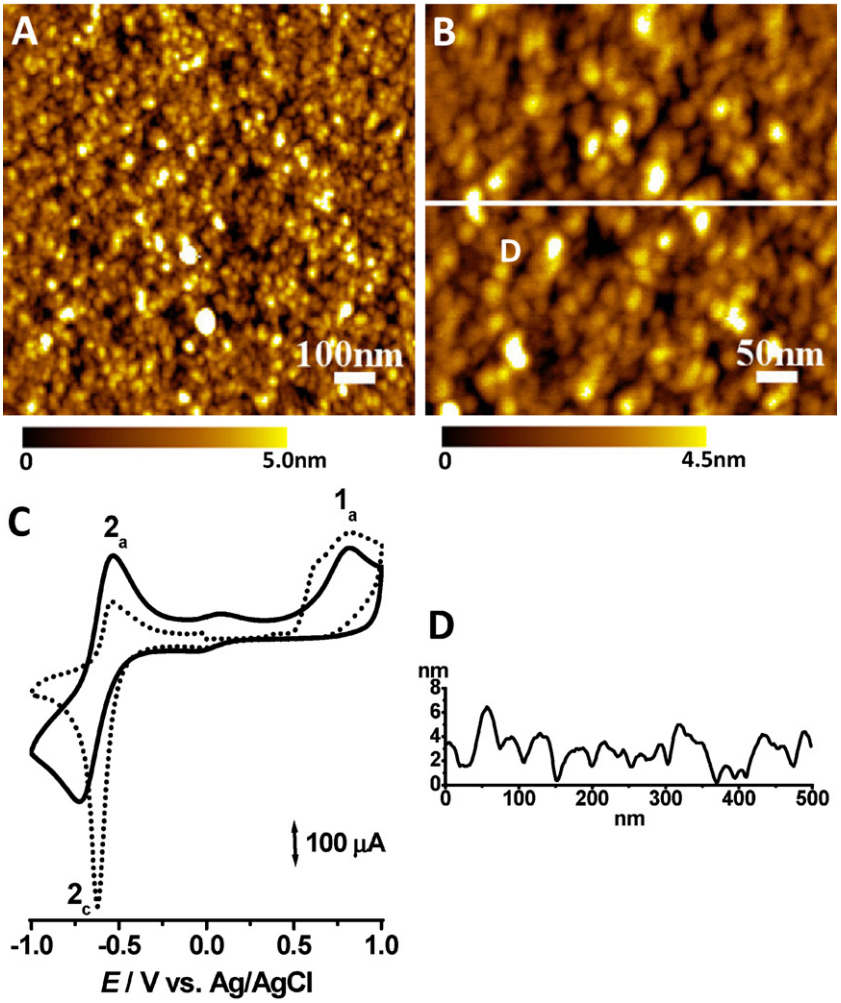

Fig. 5. PNR-modified HOPG electrode. (A and B) MAC mode AFM topographical images in air, (C) electropolymerization of NR monomer at the HOPG electrode by potential cycling between −1.0 and +1.0 V, vs. AgQRE, from a solution of 1 mM NR in pH 5.5 0.05 M PB and 0.3 M KNO_3: (—) 1st and (···) 10th scan, scan rate 50 mV s^{-1}, and (D) cross-section profile through white line in image (B).

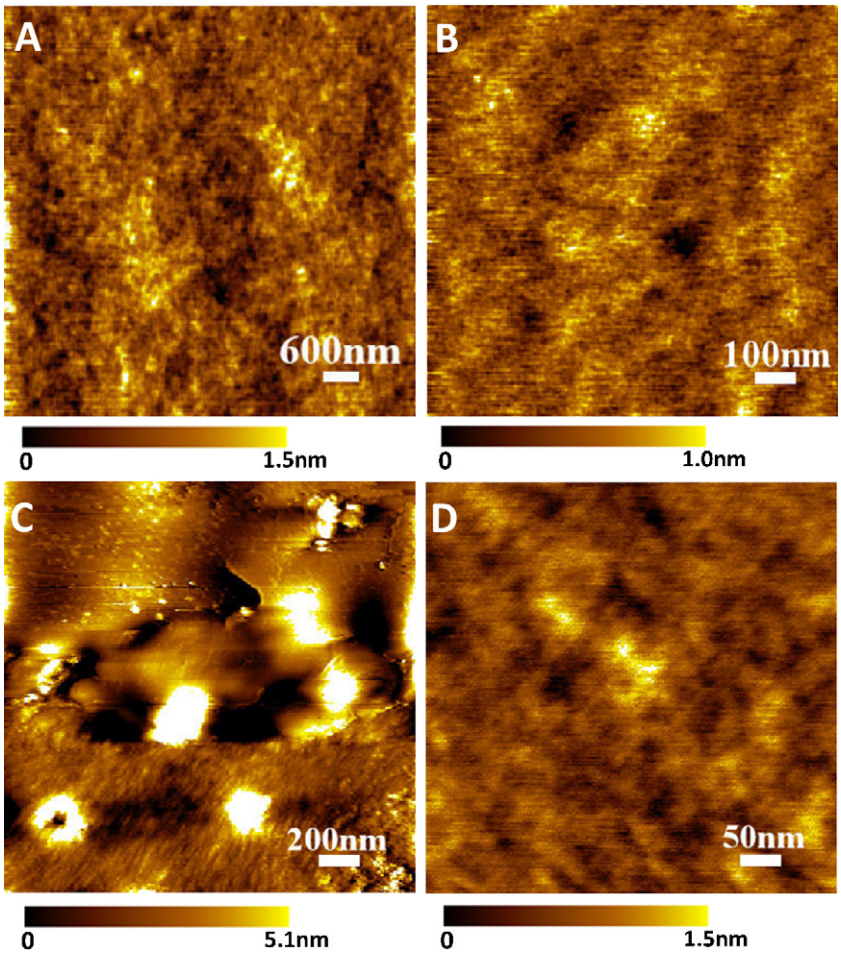

Fig. 6. (A and B) PNR redox mediator GOPMOS sol–gel-modified HOPG electrode (PNR/GOPMOS) and (C and D) with encapsulated glucose oxidase (PNR/GOPMOS–GOx). MAC mode AFM topographical images in air.

Fig. 4A–C. Indeed, the PNR/GOPMOS network showed a very low RMS roughness of only 0.3 nm, for a 1000 nm × 1000 nm image, Fig. 6B.

Finally, AFM was used to image a GPMOS–GOx film placed on top of a PNR-modified HOPG electrode, *Procedure 4*, reproducing the method of preparation of PNR redox mediated sol–gel-GOx encapsulated glucose biosensors on carbon electrode substrates.

The PNR/GOPMOS–GOx films obtained, Fig. 6C, were very non-uniform, due to an inhomogeneous distribution of the enzyme in the GOPMOS film. It was previously found that the PNR redox mediator deposited onto the carbon electrode dissolves to a small extent in the GOPMPOS–GOx solution dropped onto the PNR-modified HOPG electrode (Pauliukaite et al., 2007), mixing into the network formed, which could change the morphological characteristics of the assembly. In fact, after characterizing the changes of external roughness of the PNR/GOPMOS–GOx-modified HOPG electrode it was observed that large areas of the film were extremely smooth, ~0.3 nm RMS roughness, Fig. 6D.

4. Discussion

Sol–gel networks prepared on the HOPG electrode surface, using four different oxysilane precursors: MTMOS, TEOS, APTOS and GOPMOS, were studied at room temperature in air. MAC mode AFM characterized the surface morphological features of the immobilised sol–gel networks, representing a useful semi-quantitative method to determine the relative extent of pore formation on the deposition patterns of different sol–gel films. The topographical characteristics of each sol–gel film, including the roughness, size and apparent distribution of pores, depended not only on differences in the oxysilane precursor chemical structure, but also on the composition of the sol–gel precursor mixture, described in *Procedure 1*.

The formation of sol–gel films from the oxysilane precursors involves a two-step gelation process, sol–gel hydrolysis and polycondensation reaction. The rate of the polycondensation reaction mechanism of the gelation process is an important factor influencing the sol–gel pattern of adsorption. The APTOS and GOPMOS sol–gel mixtures have approximately the same rate of polycondensation, faster than that of the MTMOS sol–gel mixture, which in turn is faster than of the TEOS sol–gel mixture. The rate of the polycondensation reaction mechanisms follows the sequence: TEOS < MTMOS < GOPMOS ≈ APTOS.

The TEOS sol–gel film had the slowest gelation process, corresponding to a slow-rate polycondensation reaction mechanism, and led to the formation of an incomplete network, therefore less suitable for good encapsulation of enzymes, as is shown on the surface of HOPG, for both 5 min, Fig. 2A, and 1 h, Fig. 2B and C, deposition contact times.

MTMOS, APTOS and GOPMOS sol–gel films clearly showed the formation of pores of different sizes and morphological structures, a characteristic especially important for the entrapment of enzymes in the sol–gel lattice, Figs. 1, 3 and 4, TEOS being the exception. The MTMOS sol–gel film showed an RMS roughness of 1.0 nm, with both small and large pores, the latter being able to cause easy enzyme leakage.

The formation of more stable, smoother sol–gel films, through a faster gelation process, of only 0.4 nm RMS roughness, and with a dense and uniform distribution of narrow pores, appropriate for enzyme encapsulation, was successfully achieved using sol–gel mixtures containing APTOS or GOPMOS. However, whilst in the case of APTOS sol–gel a small number of large pores was still present, the GOPMOS sol–gel film surface showed no large pores, essential for good entrapment of the enzymes and, additionally, not allowing the enzymes to leach, suggesting a reduced need for an inert external protective polymer membrane, such as those developed in (Pauliukaite et al., 2008). Moreover, due to the length of the glycidoxypropyl groups, the GOPMOS sol–gel film pores are sufficiently large to preserve a good enzyme conformation mobility and electrocatalytic activity.

All the topographical differences with respect to porosity between the MTMOS, TEOS, APTOS and GOPMOS sol–gel films observed in the AFM images explain earlier electrochemical data obtained with biosensors prepared by encapsulating GOx into the sol–gel layers (Pauliukaite and Brett, 2005; Pauliukaite et al., 2006). The best enzyme immobilisation in the sol–gel films and electrochemical response to glucose, i.e. the highest sensitivity, the lowest limit of detection and the highest stability in time, for the previously optimised biosensors (Pauliukaite and Brett, 2005; Pauliukaite et al., 2006) have been observed for GOPMOS, followed by APTOS and least for MTMOS and TEOS.

HOPG electrodes modified by electrochemically-deposited PNR as mediator and GOPMOS sol–gel with encapsulated GOx were also characterized. PNR-modified HOPG showed a surface covered by globular aggregates, Fig. 5. The PNR/GOPMOS and PNR/GOPMOS–GOx films on the HOPG surface were smoother and with narrower pores, Fig. 6, than the GOPMOS and GOPMOS–GOx films, Fig. 4. This can be explained because the PNR mediator deposited onto the carbon electrode surface dissolves to a small extent in the oxysilane solution during gelation (Pauliukaite et al., 2007), and becomes incorporated in the sol–gel network formed, leading to a PNR/sol–gel film with different morphological characteristics. In fact, the epoxy ring present at the end of the glycidoxy group of the GOPMOS may react with the amino groups present in the PNR (Gao et al., 2004), enhancing the hydrophobic interaction between the GOPMOS and the aromatic rings of PNR, and leading to the formation of a more compact and smoother polymeric film.

5. Conclusions

The morphology of silica sol–gel films with encapsulated enzyme and redox mediator on HOPG electrode surfaces was investigated. The chemical structure of the oxysilane precursors and the composition of the sol–gel mixture influenced the roughness, the size and the distribution of pores in the sol–gel films, which are important criteria for efficient enzyme encapsulation. The surface morphological properties of four different oxysilane sol–gel films suggest that the best conditions for the immobilisation of enzymes within their structure follow the sequence: GOPMOS > APTOS > MTMOS > TEOS. These AFM results confirm the differences in stability with time, sensitivity and limit of detection observed for electrochemical biosensor assemblies on carbon electrodes, with PNR redox mediator and sol–gel encapsulated GOx enzyme layers.

Acknowledgements

Financial support from Fundação para a Ciência e Tecnologia (FCT), Post-Doctoral Grants SFRH/BPD/27087/2006 (A.M. Chiorcea-Paquim), SFRH/BPD/27075/2006 (R. Pauliukaite), Project PTDC/QUI/65255/2006, POCI 2010 (co-financed by the European Community Fund FEDER), and ICEMS (Research Unit 103), is gratefully acknowledged.

References

Anitha, K., Mohan, S.V., Reddy, S.J., 2004. Biosens. Bioelectron. 20 (4), 848–856.
Barroso-Fernandez, B., Theresa Lee-Alvarez, M., Seliskar, C.J., Heineman, W.R., 1998. Anal. Chim. Acta 370 (2–3), 221–230.
Barsan, M.M., Pinto, E.M., Brett, C.M.A., 2008. Electrochim. Acta 53 (11), 3973–3982.
Chiorcea, A.-M., Oliveira Brett, A.M., 2004. Bioelectrochemistry 63 (1–2), 229–232.
Couto, C.M.C.M., Araujo, A.N., Montenegro, M.C.B.S.M., Rohwedder, J., Raimundo, I., Pasquini, C., 2002. Talanta 56 (6), 997–1003.
Ferrer, M.L., del Monte, F., Levy, D., 2002. Chem. Mater. 14 (9), 3619–3621.
Gao, L., Fang, Y., Wen, X., Li, Y., Hu, D., 2004. J. Phys. Chem. B 108 (4), 1207–1213.
Han, K., Wu, Z., Lee, J., Ahn, I.-S., Park, J.W., Min, B.R., Lee, K., 2005. Biochem. Eng. J. 22 (2), 161–166.
Harwood, G.W.J., Pouton, C.W., 1996. Adv. Drug Deliv. Rev. 18 (2), 163–191.
Jia, W.Z., Wang, K., Zhu, Z.J., Song, H.T., Xia, X.H., 2007. Langmuir 23 (23), 11896–11900.
Kauffmann, C.G., Mandelbaum, R.T., 1996. J. Biotechnol. 51 (3), 219–225.
Künzelmann, U., Böttcher, H., 1997. Sens. Actuators B 39 (1–3), 222–228.
Lee, W.Y., Lee, K.S., Kim, T.H., Shin, M.C., Park, J.K., 2000a. Electroanalysis 12 (1), 78–82.
Lee, W.Y., Kim, S.-R., Kim, T.-H., Lee, K.S., Shin, M.-C., Park, J.-K., 2000b. Anal. Chim. Acta 404 (2), 195–203.
Lev, O., Wu, Z., Bharathi, S., Glezer, V., Modestov, A., Gun, J., 1997. Chem. Mater. 9 (11), 2354–2375.
Li, J., Tan, S.N., Oh, J.T., 1998. J. Electroanal. Chem. 448 (1), 69–77.
Martinez-Perez, D., Ferrer, M.L., Mateo, C.R., 2003. Anal. Biochem. 322 (2), 238–242.
Nadzhafova, O., Etienne, M., Walcarius, A., 2007. Electrochem. Commun. 9 (5), 1189–1195.
Navas Diaz, A., Ramos Peinado, M.C., Torijas Minguez, M.C., 1998. Anal. Chim. Acta 363 (2–3), 221–227.
Noguer, T., Szydlowska, D., Marty, J.L., Trjanowicz, M., 2004. Pol. J. Chem. 78 (9), 1679–1689.
Noguer, T., Tencaliec, A., Calas-Blanchard, C., Avramescu, A., Marty, J.L., 2002. J. AOAC Int. 85 (6), 1383–1389.
Pamidi, P.V.A., Parrado, C., Kane, S.A., Wang, J., Smyth, M.R., Pingarron, J., 1997. Talanta 44 (11), 1929–1934.
Pauliukaite, R., Brett, C.M.A., 2005. Electrochim. Acta 50 (25–26), 4973–4980.
Pauliukaite, R., Chiorcea Paquim, A.M., Oliveira Brett, A.M., Brett, C.M.A., 2006. Electrochim. Acta 52 (1), 1–8.
Pauliukaite, R., Ghica, M.E., Barsan, M., Brett, C.M.A., 2007. J. Solid State Electrochem. 11 (7), 899–908.
Pierre, A.C., 2004. Biocatal. Biotransform. 22 (3), 145–170.
Pauliukaite, R., Schoenleber, M., Vadgama, P., Brett, C.M.A., 2008. Anal. Bioanal. Chem. 390 (4), 1121–1131.
Rabinovich, L., Lev, O., 2001. Electroanalysis 13 (4), 265–275.
Tan, X.C., Tian, Y.X., Cai, P.X., Zou, X.Y., 2005. Anal. Bioanal. Chem. 381 (2), 500–507.
Teh, H.F., Yang, X., Gong, H., Tan, S.N., 2004. Electroanalysis 16 (9), 769–773.
Tsai, H.-C., Doong, R.-A., Chiang, H.-C., Chen, K.-T., 2003. Anal. Chim. Acta 481 (1), 75–84.
Tsionsky, M., Gun, G., Glezer, V., Lev, O., 1994. Anal. Chem. 66 (10), 1747–1753.
van Unen, D.J., Engbersen, J.F.J., Reinhoudt, D.N., 2001. Biotechnol. Bioeng. 75 (2), 154–158.
Walcarius, A., 2001. Chem. Mater. 13 (10), 3351–3372.
Wang, B., Dong, S., 2000a. J. Electroanal. Chem. 487 (1), 45–50.
Wang, B., Zhang, J., Cheng, G., Dong, S., 2000. Chem. Commun. 2000 (21), 2123–2124.
Wang, J., Pamidi, P.V.A., Park, D.S., 1996. Anal. Chem. 68 (15), 2705–2708.
Yao, T., Takashima, K., 1998. Biosensens. Bioelectron. 13 (1), 67–73.
Yao, T.S., Harada, I., Nakahara, T., 1995. Bunseki Kugaku 44, 927–932.
Zhang, S., Wang, N., Niu, Y., Sun, C., 2005. Sens. Actuators B 109 (2), 367–374.
Zhou, W., Dong, J.H., Qiu, K.Y., Wei, Y., 1999. J. Appl. Polym. Sci. 73 (3), 419–424.